Robust Fluorescent Detection of Protein Fatty-Acylation with Chemical Reporters

ARTICLE *in* JOURNAL OF THE AMERICAN CHEMICAL SOCIETY · MAY 2009

Impact Factor: 12.11 · DOI: 10.1021/ja810122f · Source: PubMed

J|A|C|S
ARTICLES

Published on Web 03/12/2009

Robust Fluorescent Detection of Protein Fatty-Acylation with Chemical Reporters

Guillaume Charron, Mingzi M. Zhang, Jacob S. Yount, John Wilson, Anuradha S. Raghavan, Eliah Shamir, and Howard C. Hang*

The Laboratory of Chemical Biology and Microbial Pathogenesis, The Rockefeller University, New York, New York 10065

Received December 29, 2008; E-mail: hhang@mail.rockefeller.edu

Abstract: Fatty-acylation of proteins in eukaryotes is associated with many fundamental cellular processes but has been challenging to study due to limited tools for rapid and robust detection of protein fatty-acylation in cells. The development of azido-fatty acids enabled the nonradioactive detection of fatty-acylated proteins in mammalian cells using the Staudinger ligation and biotinylated phosphine reagents. However, the visualization of protein fatty-acylation with streptavidin blotting is highly variable and not ideal for robust detection of fatty-acylated proteins. Here we report the development of alkynyl-fatty acid chemical reporters and improved bioorthogonal labeling conditions using the Cu^{I}-catalyzed Huisgen [3 + 2] cycloaddition that enables specific and sensitive fluorescence detection of fatty-acylated proteins in mammalian cells. These improvements allow the rapid and robust biochemical analysis of fatty-acylated proteins expressed at endogenous levels in mammalian cells by in-gel fluorescence scanning. In addition, alkynyl-fatty acid chemical reporters enable the visualization of fatty-acylated proteins in cells by fluorescence microscopy and flow cytometry. The ability to rapidly visualize protein fatty-acylation in cells using fluorescence detection methods therefore provides new opportunities to interrogate the functions and regulatory mechanisms of fatty-acylated proteins in physiology and disease.

Introduction

Protein fatty-acylation regulates diverse biological processes in eukaryotes ranging from cellular growth and differentiation to lymphocyte activation and synaptic transmission.[1] Fatty acid modifications target proteins to discrete membrane compartments, thus enabling spatial and temporal regulation of complex signaling pathways.[1] The two major forms of protein fatty-acylation in eukaryotes are *N*-myristoylation and *S*-palmitoylation, characterized by the attachment of myristic acid (14:0) or palmitic acid (16:0) to proteins (Figure 1A). Myristoylation occurs predominantly on N-terminal glycine residues that are cotranslationally installed on nascent polypeptides by *N*-myristoyltransferases (NMTs).[2] Structural studies of yeast NMT revealed a well-defined binding site for myristoyl-CoA that provides a molecular ruler to discriminate against longer-chain fatty-acyl-CoA substrates.[3,4] *N*-myristoylation also occurs post-translationally as proteolytic cleavage of protein substrates can reveal *de novo* glycine residues at the N-terminus of proteins for fatty-acylation.[5] *S*-Palmitoylation or *S*-acylation of proteins on the other hand is a reversible modification that takes place on the thiol side chain of cysteine residues.[6] *S*-Palmitoylation is mediated by a family of DHHC-containing protein acyltransferases (DHHC-PATs) for which no primary amino acid consensus sequence has emerged for their protein substrates.[7] In addition to intracellular proteins, fatty-acylation can also occur on secreted growth factors and dramatically influence their extracellular signaling properties in tissues.[8] Interestingly, fatty-acylation has also been discovered on serine residues of secreted growth factors such as Wnt.[9] While many fatty-acylated proteins have been identified and are associated with various cellular pathways, their specific functions and mechanisms of regulation in physiology and disease remain to be explored.

The diversity and abundance of protein fatty-acylation in eukaryotes as well as their regulatory mechanisms have been difficult to study due to limited methods for analyzing protein lipidation.[10] Detection of protein fatty-acylation in cells is typically performed by metabolic labeling with radioactive (^{3}H or ^{14}C) fatty acids followed by visualization of purified proteins or cell lysates using autoradiography.[10] While effective, radioactivity often requires days to weeks to visualize fatty-acylated proteins. Radioactive ^{125}iodinated-fatty acids improve the detection of fatty-acylated proteins by autoradiography, but these

(1) Resh, M. D. *Nat. Chem. Biol.* **2006**, *2*, 584–590.
(2) Farazi, T. A.; Waksman, G.; Gordon, J. I. *J. Biol. Chem.* **2001**, *276*, 39501–3954.
(3) Farazi, T. A.; Waksman, G.; Gordon, J. I. *Biochemistry* **2001**, *40*, 6335–6343.
(4) Bhatnagar, R. S.; Futterer, K.; Farazi, T. A.; Korolev, S.; Murray, C. L.; Jackson-Machelski, E.; Gokel, G. W.; Gordon, J. I.; Waksman, G. *Nat. Struct. Biol.* **1998**, *5*, 1091–1097.
(5) de Jonge, H. R.; Hogema, B.; Tilly, B. C. *Sci. STKE* **2000**, *2000* (63), 1.
(6) Linder, M. E.; Deschenes, R. J. *Nat. Rev. Mol. Cell Biol.* **2007**, *8*, 74–84.
(7) Mitchell, D. A.; Vasudevan, A.; Linder, M. E.; Deschenes, R. J. *J. Lipid Res.* **2006**, *47*, 1118–1127.
(8) Mann, R. K.; Beachy, P. A. *Annu. Rev. Biochem.* **2004**, *73*, 891–923.
(9) Takada, R.; Satomi, Y.; Kurata, T.; Ueno, N.; Norioka, S.; Kondoh, H.; Takao, T.; Takada, S. *Dev. Cell* **2006**, *11*, 791–801.
(10) Resh, M. D. *Methods* **2006**, *40*, 191–197.

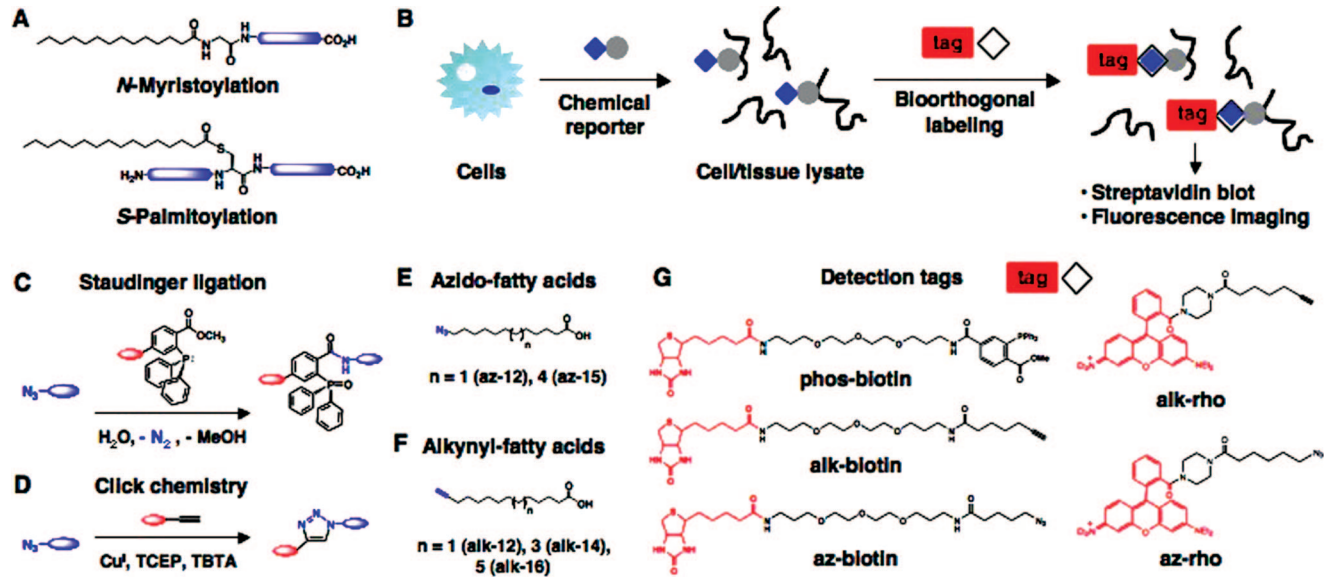

Figure 1. Analysis of protein fatty-acylation with chemical reporters. (A) *N*-Myristoylation and *S*-palmitoylation. (B) Metabolic labeling of mammalian cells with chemical reporters and bioorthogonal labeling of proteins. Bioorthogonal labeling methods: (C) Staudinger ligation and (D) Cu^{I}-catalyzed Huisgen [3 + 2] cycloaddition or "click chemistry" enable selective covalent attachment of detection tags to azide/alkyne-modified substrates. Chemical reporters: (E) Azido-fatty acids. (F) Alkynyl-fatty acids. (G) Detection tags.

reagents are hazardous, cumbersome and not readily available.[11,12] To circumvent the limitations of radiolabeled fatty acids, the acyl−biotin exchange (ABE) protocol developed by Drisdel and Green affords a nonradioactive means to visualize *S*-palmitoylated proteins by streptavidin blot.[13] The combination of ABE with mass spectrometry-based proteomics using multidimensional protein identification technology (MudPIT) to yeast[14] and neurons[15] has recently revealed many new *S*-palmitoylated proteins in eukaryotes. Alternatively, we have developed chemical reporters of protein fatty-acylation that enable rapid nonradioactive detection of *N*-myristoylated and *S*-palmitoylated proteins from mammalian cells using bioorthogonal labeling methods (Figure 1B).[16] This chemical approach involves metabolic labeling of cells with azido-fatty acid analogues (Figure 1E) followed by reaction of azide-modified proteins with chemoselective detection tags, such as phosphine-biotin via the Staudinger ligation (Figure 1C) and visualization of biotinylated-polypeptides by streptavidin blot.[16] This two-step labeling method appears to be quite general, as we and other laboratories have employed this strategy to visualize fatty-acylation of diverse proteins,[16−20] including secreted proteins such as Wnt.[21] The selective biotinylation with ABE[13] or azido-fatty acids/phosphine-biotin[16−21] provides a convenient means to visualize fatty-acylated proteins; however, immunoblotting methods are not ideal for analyzing quantitative changes in protein fatty-acylation necessary for investigating dynamics or regulatory mechanisms. Here we report the robust fluorescent detection of fatty-acylated proteins with chemical reporters that enable rapid biochemical analysis as well as imaging of protein fatty-acylation in mammalian cells.

Results

Comparative Analysis of Bioorthogonal Labeling Methods. Advances in bioorthogonal labeling methods employing the Cu^{I}-catalyzed Huisgen [3 + 2] cycloaddition or "click chemistry" reaction between alkyl azides and alkynes (Figure 1D),[22−28] suggested an opportunity to improve the analysis of fatty-acylated proteins with chemical reporters. We therefore synthesized a series of alkynyl-fatty acids of different lengths (Figure 1F and Supporting Information, Figure S1) as potential chemical reporters as well as a panel of biotinylated (alk-biotin, az-biotin) and fluorescent (alk-rho, az-rho) detection tags (Figure 1G and Supporting Information, Figure S1) to explore the detection of fatty-acylated proteins with click chemistry.

(11) Berthiaume, L.; Peseckis, S. M.; Resh, M. D. *Methods Enzymol.* **1995**, *250*, 454–466.
(12) Peseckis, S. M.; Deichaite, I.; Resh, M. D. *J. Biol. Chem.* **1993**, *268*, 5107–5114.
(13) Drisdel, R. C.; Green, W. N. *Biotechniques* **2004**, *36*, 276–285.
(14) Roth, A. F.; Wan, J.; Bailey, A. O.; Sun, B.; Kuchar, J. A.; Green, W. N.; Phinney, B. S.; Yates, J. R., 3rd; Davis, N. G. *Cell* **2006**, *125*, 1003–1013.
(15) Kang, R.; Wan, J.; Arstikaitis, P.; Takahashi, H.; Huang, K.; Bailey, A. O.; Thompson, J. X.; Roth, A. F.; Drisdel, R. C.; Mastro, R.; Green, W. N.; Yates, J. R., 3rd.; Davis, N. G.; El-Husseini, A. *Nature* **2008**, *456*, 904–909.
(16) Hang, H. C.; Geutjes, E. J.; Grotenbreg, G.; Pollington, A. M.; Bijlmakers, M. J.; Ploegh, H. L. *J. Am. Chem. Soc.* **2007**, *129*, 2744–2745.
(17) Heal, W. P.; Wickramasinghe, S. R.; Bowyer, P. W.; Holder, A. A.; Smith, D. F.; Leatherbarrow, R. J.; Tate, E. W. *Chem. Commun. (Cambridge)* **2008**, 480–482.
(18) Heal, W. P.; Wickramasinghe, S. R.; Leatherbarrow, R. J.; Tate, E. W. *Org. Biomol. Chem.* **2008**, *6*, 2308–2315.
(19) Kostiuk, M. A.; Corvi, M. M.; Keller, B. O.; Plummer, G.; Prescher, J. A.; Hangauer, M. J.; Bertozzi, C. R.; Rajaiah, G.; Falck, J. R.; Berthiaume, L. G. *FASEB J.* **2008**, *22*, 721–732.
(20) Martin, D. D.; Vilas, G. L.; Prescher, J. A.; Rajaiah, G.; Falck, J. R.; Bertozzi, C. R.; Berthiaume, L. G. *FASEB J.* **2008**, *22*, 797–806.
(21) Ching, W.; Hang, H. C.; Nusse, R. *J. Biol. Chem.* **2008**, *283*, 17092–17098.
(22) Wang, Q.; Chan, T. R.; Hilgraf, R.; Fokin, V. V.; Sharpless, K. B.; Finn, M. G. *J. Am. Chem. Soc.* **2003**, *125*, 3192–3193.
(23) Rostovtsev, V. V.; Green, L. G.; Fokin, V. V.; Sharpless, K. B. *Angew. Chem., Int. Ed.* **2002**, *41*, 2596–2599.
(24) Tornoe, C. W.; Christensen, C.; Meldal, M. *J. Org. Chem.* **2002**, *67*, 3057–3064.
(25) Speers, A. E.; Adam, G. C.; Cravatt, B. F. *J. Am. Chem. Soc.* **2003**, *125*, 4686–4687.
(26) Speers, A. E.; Cravatt, B. F. *J. Am. Chem. Soc.* **2005**, *127*, 10018–10019.
(27) Weerapana, E.; Speers, A. E.; Cravatt, B. F. *Nat. Protoc.* **2007**, *2*, 1414–1425.
(28) Speers, A. E.; Cravatt, B. F. *Chem. Biol.* **2004**, *11*, 535–546.

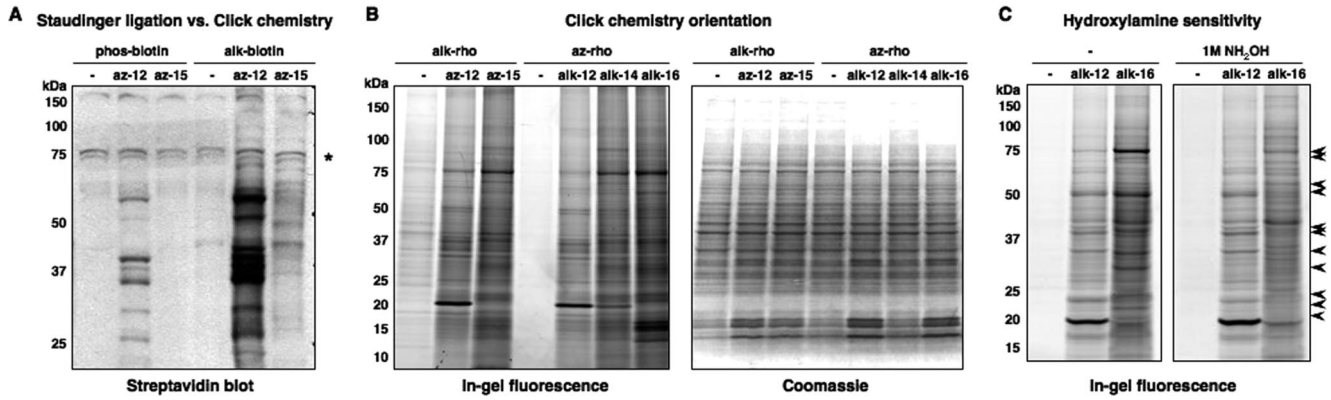

Figure 2. Biochemical analysis of chemical reporters for protein fatty-acylation in mammalian cells. (A) Staudinger ligation versus click chemistry. (*) Indicates comparable levels of endogenously biotinylated proteins. (B) Alkyne/azide orientation comparative analysis of protein fatty-acylation with click chemistry by in-gel fluorescence scanning. Comparable levels of protein loading were demonstrated by Coomassie staining of the gel. (C) Hydroxylamine sensitivity of proteins in Jurkat cell lysates labeled with alkynyl-fatty acids. Experiments were performed with cell lysates from Jurkat T cells metabolically labeled with DMSO (-), 20 μM azido- or alkynyl-fatty acids (az-12, az-15, alk-12, alk-14 or alk-16). Arrows highlight proteins with decreased fluorescence due to NH_2OH exposure.

Comparative analysis of the Staudinger ligation and click chemistry reaction with azido-fatty acid-labeled cell lysates and biotinylated detection probes (phos-biotin and alk-biotin, respectively) revealed significantly improved detection of fatty-acylated proteins by streptavidin blotting with the Cu^I-catalyzed Huisgen [3 + 2] cycloaddition (Figure 2A). We then investigated whether the orientation of alkyne and azide functional groups would influence the overall sensitivity of fatty-acylated protein analysis using click chemistry. Cells were metabolically labeled with azide- or alkynyl-analogues of myristic acid (az-12, alk-12) or palmitic acid (az-15, alk-14, alk-16) and assayed for the specific detection of fatty-acylated proteins in cell lysates using biotin (alk-biotin, az-biotin) or fluorescence (alk-rho, az-rho) detection tags and streptavidin blotting (Supporting Information, Figure S2) or in-gel fluorescence scanning (Figure 2B), respectively. Profiles of fatty-acylated proteins visualized by in-gel fluorescence scanning revealed substantially more proteins compared to streptavidin blotting, particularly with the palmitic acid analogues (az-15, alk-14 and alk-16). Like their azide counterparts, the alkynyl-fatty acids (alk-12, alk-14 and alk-16) functioned as efficient chemical reporters of protein fatty-acylation and exhibited chain length-dependent protein labeling (Figure 2B). The similar profiles of fatty-acylated proteins visualized by azido- or alkynyl-fatty acid metabolic labeling and click chemistry in-gel fluorescence analysis reinforce the concept that the small azide and alkyne chemical reporters afford efficient tools to visualize protein fatty-acylation in cells (Figure 2B). Comparative analysis of fatty-acylated proteins visualized by in-gel fluorescence scanning demonstrated that alkynyl-fatty acid chemical reporters, in combination with the azido-rhodamine (az-rho) detection tag, improve the sensitivity of bioorthogonal labeling compared to the reverse click chemistry orientation owing to lower background signal (Figure 2B and Supporting Information, Figure S2D). These observations are consistent with other studies using alkyne- or azide-functionalized chemical probes.[28,29]

Specificity and Generality of Fatty-Acylated Protein Labeling with Chemical Reporters. Having established robust fluorescence detection of proteins metabolically labeled with alkynyl-fatty acid chemical reporters, we determined their kinetics and specificity of labeling fatty-acylated proteins in cells. Time- and dose-dependent analyses of metabolic labeling with the alkynyl-fatty acids revealed that the click chemistry and in-gel fluorescence imaging protocol required shorter labeling time (minutes) and lower concentrations of fatty acid chemical reporters to robustly detect fatty-acylated proteins compared to streptavidin blotting[6] (Supporting Information, Figure S3). Competition of alkynyl-fatty acid protein labeling (alk-12, alk-14 and alk-16) with naturally occurring fatty acids revealed that alk-12 protein labeling is preferentially blocked by myristic acid, whereas alk-14 and alk-16 protein labeling is most effectively reduced by palmitic acid (Supporting Information, Figure S4). Inhibition of protein synthesis with cycloheximide (CHX) abrogated the metabolic labeling of several prominent polypeptides by alk-12 (Supporting Information, Figure S5A). Most proteins targeted by alk-12, alk-14 and alk-16 were resistant to CHX treatment, however, suggesting fatty-acylation of these protein substrates occurs posttranslationally (Supporting Information, Figure S5A). Coincubation of the alkynyl-fatty acids with 2-hydroxymyristic acid (HMA), a reported *N*-myristoylation inhibitor,[30] selectively blocked alk-12 protein labeling compared to alk-14 and alk-16 (Supporting Information, Figure S5B). In contrast, addition of 2-bromopalmitic acid (2-BP), a nonspecific *S*-palmitoylation inhibitor,[31] at concentrations that did not induce cell death reduced protein labeling with alk-12, alk-14 and alk-16 (Supporting Information, Figure S5C). To differentiate between *N*-myristoylated and *S*-acylated proteins, az-rho-modified alkynyl-fatty acid-labeled cell lysates were subjected to in-gel treatment with hydroxylamine (NH_2OH),[13] which preferentially cleaves thioesters at neutral pH and is the key step of ABE. The fluorescent signals of alkynyl-fatty acid-labeled proteins were reduced after in-gel exposure to NH_2OH; however, the CHX-sensitive proteins labeled by alk-12 were resistant to NH_2OH cleavage (Figure 2C). These experiments suggest that alk-12 cotranslationally targets *N*-myristoylated proteins (CHX-sensitive and NH_2OH-resistant) as well as *S*-acylated proteins (CHX-resistant and NH_2OH-sensitive), whereas alk-16 preferentially labels *S*-acylated proteins in cell lysates. Protein labeling with alk-14

(29) Agard, N. J.; Baskin, J. M.; Prescher, J. A.; Lo, A.; Bertozzi, C. R. *ACS Chem. Biol.* **2006**, *1*, 644–648.
(30) Paige, L. A.; Zheng, G. Q.; DeFrees, S. A.; Cassady, J. M.; Geahlen, R. L. *Biochemistry* **1990**, *29*, 10566–10573.
(31) Webb, Y.; Hermida-Matsumoto, L.; Resh, M. D. *J. Biol. Chem.* **2000**, *275*, 261–270.

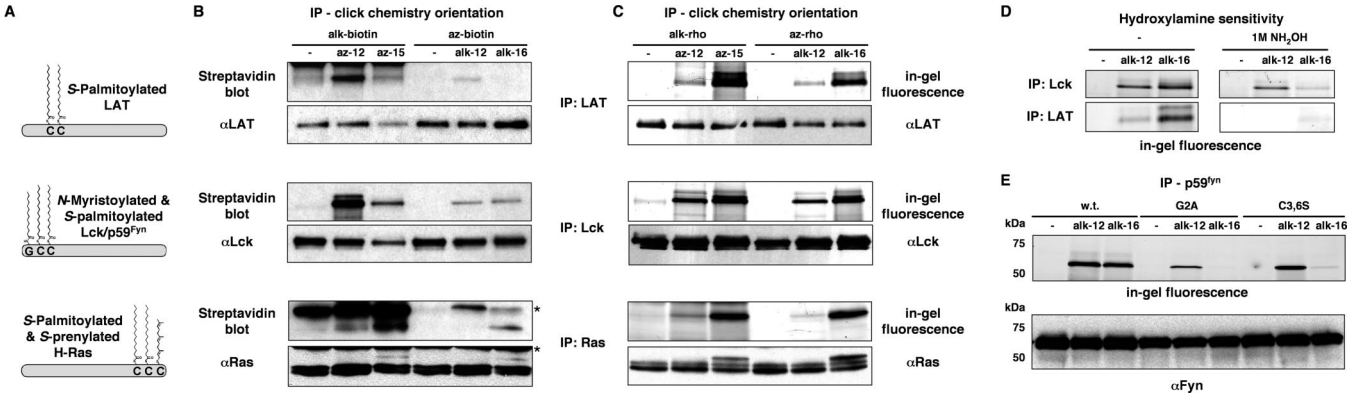

Figure 3. Robust visualization of fatty-acylated proteins after immunoprecipitation. (A) Schematic representation of lipidation sites for LAT (*S*-palmitoyl-Cys26, *S*-palmitoyl-Cys29), Lck (*N*-myristoyl-Gly2, *S*-palmitoyl-Cys3, *S*-palmitoyl-Cys5), H-Ras (*S*-palmitoyl-Cys181, *S*-palmitoyl-Cys184, *S*-prenyl-Cys186) and Fyn (*N*-myristoyl-Gly2, *S*-palmitoyl-Cys3, *S*-palmitoyl-Cys6), examples of different classes of fatty-acylated proteins. (B) Comparative analysis of click chemistry orientation with Lck, LAT and Ras by streptavidin blotting. (*) Indicates nonspecific cross-reactivity of streptavidin or anti-mouse secondary antibody with light-chain of anti-Ras antibody. (C) Comparative analysis of click chemistry orientation with Lck, LAT and Ras by in-gel fluorescence scanning. (D) Hydroxylamine sensitivity of alkynyl-fatty acid Lck and LAT labeling. Experiments were performed with cell lysates from Jurkat T cells metabolically labeled with DMSO (-), 20 μM azido- or alkynyl-fatty acids (az-12, az-15, alk-12, or alk-16). (E) Comparative analysis of acylation state of wild-type, G2A mutant and C3,6S mutant Fyn. HeLa cells were metabolically labeled with DMSO (-) or alkynyl-fatty acids (20 μM alk-12 or alk-16). Comparable protein load was demonstrated by blotting for the corresponding proteins.

appears to represent a combination of alk-12 and alk-16 labeling, which is consistent with previous metabolic labeling experiments using az-14, an azido-fatty acid analogue bearing 14-carbons.[16]

We further evaluated the efficiency and specificity of our chemical reporters in the detection of different classes of fatty-acylated proteins: *N*-myristoylated and *S*-palmitoylated - Lck[32] and Fyn,[33] *S*-palmitoylated only - Linker for Activation of T Cells (LAT),[34] and *S*-palmitoylated and *S*-prenylated - Ras[35] (Figure 3A). For these studies, Jurkat cells were metabolically labeled with azido- (az-12, az-15) or alkynyl- (alk-12, alk-16) fatty acids. Proteins of interest were immunoprecipitated from cell lysates, subjected to click chemistry with biotinylated (alk-biotin, az-biotin) or fluorescent (alk-rho, az-rho) detection tags prior to visualization by streptavidin blot (Figure 3B) or in-gel fluorescence scanning (Figure 3C), respectively. As with cell lysates, in-gel fluorescence detection of the immunopurified fatty-acylated proteins (Lck, LAT and Ras) was markedly improved compared to streptavidin blotting and alkynyl-fatty acids/azido-rhodamine afforded the optimal signal-to-noise for fluorescent detection (Figure 3B,C). For example, *S*-acylation of LAT was observed with myristic acid analogues (az-12, alk-12) and nearly undetectable using palmitic acid analogues (az-15, alk-16) by streptavidin blotting (Figure 3B, top panels), but was robustly visualized by in-gel fluorescence scanning (Figure 3C, top panels). Similar observations were obtained with Lck and Ras (Figure 3B,C, middle and bottom panels). Although it is unclear why the detection of *S*-acylated proteins is more efficient with myristic acid analogues (az-12, alk-12) compared to palmitic acid analogues (az-15, alk-16) by streptavidin blotting, direct in-gel fluorescence detection affords more consistent, reproducible and specific visualization of fatty-acylated proteins that avoids any variability associated with immunoblotting of hydrophobic lipidated proteins (Figure 3B,C).

Fatty acid chemical reporters combined with fluorescence detection enables specific detection of *N*-myristoylated and *S*-palmitoylated proteins. Fatty-acylation of Lck, a *N*-myristoylated and *S*-palmitoylated protein, was readily observed with myristic acid (az-12 and alk-12) and palmitic acid (az-15, alk-16) chemical reporters, whereas LAT and Ras, *S*-palmitoylated proteins without N-terminal Gly residues, were more prominently labeled with palmitic acid chemical reporters (az-15, alk-16) (Figure 3C). The low levels of LAT and Ras labeling with az-12 and alk-12 is consistent with our experiments with cell lysates (Figure 2B,C), which further demonstrates that myristic acid analogues can be incorporated onto *S*-acylated proteins, albeit less efficiently than longer chain fatty acids. These observations are not unexpected, as *S*-acylation is known to involve a heterogeneous composition of fatty acids.[36] In-gel NH_2OH treatment of alkynyl-fatty acid labeled Lck and LAT reduced the fluorescent signal derived from alk-16 on both proteins, but did not alter the alk-12 labeling of Lck (Figure 3D). We also analyzed the specificity of our fatty acid chemical reporters with wild-type and mutant constructs of p59 Fyn,[33] a well-characterized *N*-myristoylated and *S*-palmitoylated Src-family kinase, by overexpression in HeLa cells, metabolic labeling and immunoprecipitation (Figure 3E). Fatty-acylation of wild-type Fyn is readily detected with alk-12 and alk-16 labeling, whereas the *N*-myristoylation G2A mutant exhibited significantly reduced alk-12 labeling and was undetectable with alk-16 (Figure 3E). The dual *S*-palmitoylation-deficient C3,6S mutant Fyn was efficiently labeled with alk-12 and not with alk-16 (Figure 3E). These results are quantitatively identical to previously described experiments using radiolabeled fatty acids, which also demonstrated residual labeling of G2A mutant Fyn with a ^{125}I-myristic acid analogue and no labeling with ^{125}I-palmitic acid analogue.[33,37] Our experiments therefore also support the model that *N*-myristoylation precedes *S*-palmitoylation and highlight the possibility of fatty-acylation at N-terminal alanine residues. In contrast to LAT, Lck, Ras and Fyn,

(32) Paige, L. A.; Nadler, M. J.; Harrison, M. L.; Cassady, J. M.; Geahlen, R. L. *J. Biol. Chem.* **1993**, *268*, 8669–8674.
(33) Alland, L.; Peseckis, S. M.; Atherton, R. E.; Berthiaume, L.; Resh, M. D. *J. Biol. Chem.* **1994**, *269*, 16701–16705.
(34) Zhang, W.; Trible, R. P.; Samelson, L. E. *Immunity* **1998**, *9*, 239–246.
(35) Hancock, J. F.; Magee, A. I.; Childs, J. E.; Marshall, C. J. *Cell* **1989**, *57*, 1167–1177.
(36) Liang, X.; Lu, Y.; Wilkes, M.; Neubert, T. A.; Resh, M. D. *J. Biol. Chem.* **2004**, *279*, 8133–9.
(37) Liang, X.; Nazarian, A.; Erdjument-Bromage, H.; Bornmann, W.; Tempst, P.; Resh, M. D. *J. Biol. Chem.* **2001**, *276*, 30987–30994.

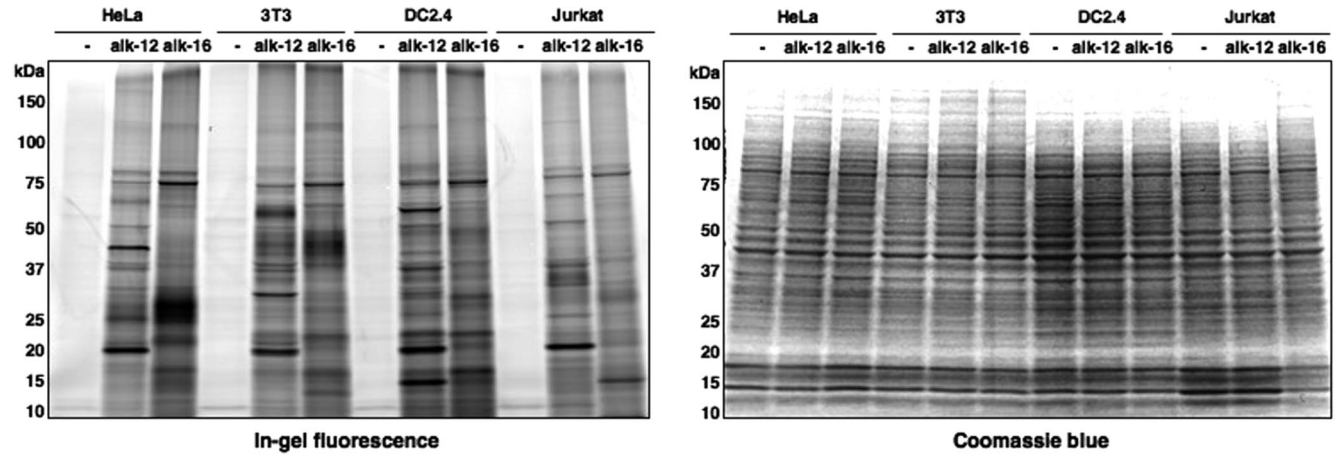

Figure 4. Profile of fatty-acylated proteomes in different cell lines. Fatty-acylated proteins from mammalian cell lines (HeLa, 3T3, DC2.4 or Jurkat T cells) metabolically labeled with DMSO (-) or alkynyl-fatty acids (20 μM alk-12 or 200 μM alk-16) and analyzed as described in Figure 2. Comparable levels of protein loading were demonstrated by Coomassie blue staining of the gels.

no alkynyl-fatty acid labeling was observed for p53, a prominent acetylated protein for which fatty-acylation has not been reported,[38] when analyzed in parallel with LAT, Lck and Ras (Supporting Information, Figure S6). Collectively, our experiments with cell lysates and specific proteins demonstrate that alk-12 and alk-14 label *N*-myristoylated and *S*-acylated proteins, whereas longer-chain fatty acid chemical reporters such as alk-16 preferentially target *S*-acylated proteins.

The generality of our method was evaluated by labeling different mammalian cell types (HeLa, 3T3, DC2.4 and Jurkat) with alkynyl-fatty acids (alk-12 or alk-16). This comparative analysis revealed remarkably diverse profiles of fatty-acylated proteins among different cell types (Figure 4). While some fatty-acylated polypeptide bands are common among the different cell types, distinct *N*-myristoylation and *S*-palmitoylation patterns are apparent. Indeed, the repertoire of fatty-acylated proteins varies dramatically between epithelial cell lines (HeLa and NIH 3T3 fibroblasts), a monocyte-derived cell line (DC2.4) and T cells (Jurkat) (Figure 4). These experiments highlight the utility of our fatty acid chemical reporters and improved detection conditions, which demonstrate unique profiles of fatty-acylated proteins in discrete cell types that undoubtedly contribute to specific cellular properties.

Fluorescence Imaging of Fatty-Acylated Proteins in Cells. Our fatty acid chemical reporters and fluorescent detection tags also provide an opportunity to visualize the distribution of fatty-acylated proteins within individual cells by fluorescence microscopy. To explore the utility of our chemical reporters for fluorescence imaging of fatty-acylated proteins in cells, HeLa cells were metabolically labeled with azido-fatty acids (az-12 or az-15) or alkynyl-fatty acids (alk-12 or alk-16), fixed with paraformaldehyde (PFA), permeabilized with Triton X-100, subjected to click chemistry reaction with alk-rho or az-rho, respectively, and imaged by fluorescence microscopy. HeLa cells labeled with azido-fatty acids (az-12 and az-15) or alkynyl-fatty acids (alk-12 or alk-16) yielded significantly higher levels of fluorescence compared to DMSO control (Supporting Information, Figure 7F). In accord with our in-gel fluorescence analysis (Figure 2B), alkynyl-fatty acids combined with az-rho labeling affords better signal-to-noise compared to the reverse click chemistry orientation (Supporting Information, Figure 7).

To determine whether the fluorescence imaging of alk-16-labeled cells reflect lipids and/or fatty-acylated proteins, HeLa cells were fixed, not permeabilized or treated with either Tween-20, Triton X-100 or methanol (MeOH) prior to click chemistry reaction with az-rho. Flow cytometry analysis of HeLa cells demonstrated that mild detergents such as Tween-20 afford specific fluorescent detection of alk-16-labeled cells similar to nonpermeabilized samples (Figure 5A). Alternatively, permeabilization/extraction of HeLa cells with Triton X-100 or MeOH, conditions that are typically used to solubilize membranes, decreased the fluorescence detection of alk-16-labeling approximately 10-fold compared to nonpermeabilized cells (Figure 5A). The reduction in mean fluorescence intensity of alk-16-labeled cells treated with Triton X-100 or MeOH suggests that fatty acid chemical reporters not installed onto proteins are solubilized and extracted under these conditions. To confirm that Triton X-100 and MeOH effectively permeabilized and extracted membranes in our fluorescent imaging experiments, the distribution and amount of glycolipid GM_1 [Gal(β1−3)-GalNAc(β1−4)(NeuAc(α2−3)Gal(β1−4)Glc(β1−1)] was analyzed by staining with fluorescently labeled cholera toxin B (FITC-CTxB) using confocal microscopy (Figure 5B). CTxB labeled the plasma membrane in nonpermeabilized cells and stained intracellular vesicles in Tween-20 treated cells that partially colocalized with alk-16 fluorescence (Figure 5B). In contrast, Triton X-100 and MeOH permeabilized samples afforded significantly reduced CTxB staining of GM_1 in HeLa cells (Figure 5B). The residual CTxB staining in Triton X-100 treated samples is consistent with GM_1 partitioning into Triton X-100-insoluble structures, which do not appear to colocalize with alk-16 fluorescence under these conditions (Figure 5B). These experiments demonstrate that the visualization of lipid substrates targeted by fatty acid chemical reporters in cells (i.e., glycolipids or fatty-acylated proteins) is significantly influenced by permeabilization/extraction of membranes prior to fluorescence imaging. While we cannot exclude the possibility that some lipids may remain after membrane permeabilization/extraction, the majority of the alk-16 fluorescence signal in Triton X-100- or MeOH-treated cells is most likely attributed to fatty-acylated proteins.

We then determined the distribution of alk-16-labeled proteins with respect to other subcellular localization markers in HeLa cells fixed and permeabilized with Triton X-100 (Figure 6).

(38) Tang, Y.; Zhao, W.; Chen, Y.; Zhao, Y.; Gu, W. *Cell* **2008**, *133*, 612–626.

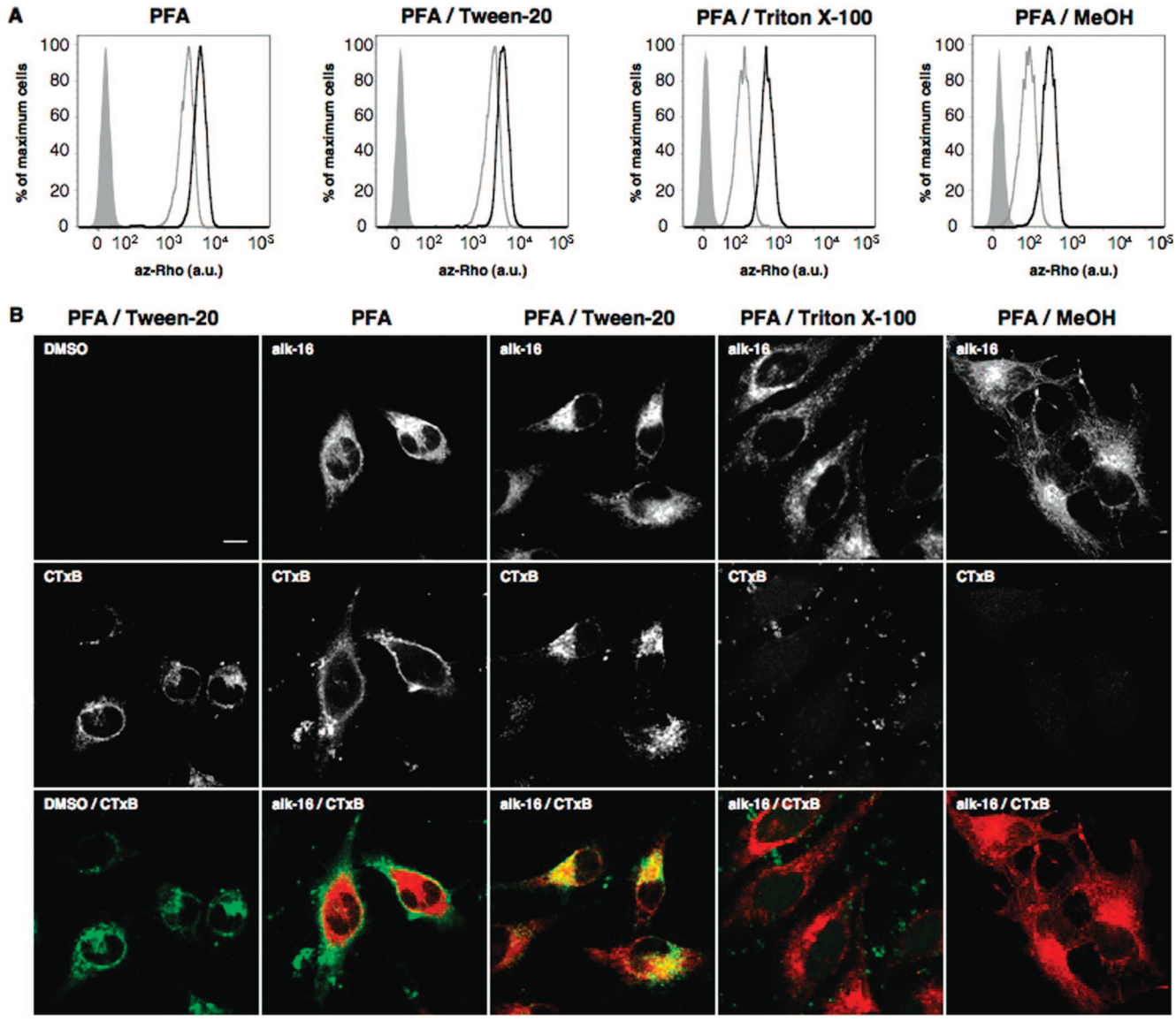

Figure 5. Effects of permeabilization on fatty-acylated protein detection in cells by flow cytometry and fluorescence microscopy. (A) HeLa cells were metabolically labeled with DMSO (shaded histogram) or alk-16 for 1 h at 20 μM (gray line) or 100 μM (black line). Cells were fixed with 3.7% PFA, permeabilized with either 1% Tween-20, 0.1% Triton X-100, −20 °C MeOH or not permeabilized. Cells were reacted with 20 μM az-rho, 1 mM TCEP, 100 μM TBTA and 1 mM $CuSO_4$, and analyzed by flow cytometry. (B) HeLa cells were metabolically labeled with DMSO or 20 μM alk-16 for 1 h. Cells were fixed with 3.7% PFA, permeabilized with either 1% Tween-20, 0.1% Triton X-100, −20 °C MeOH or not permeabilized. Cells were reacted with 20 μM az-rho, 1 mM TCEP, 100 μM TBTA, and 1 mM $CuSO_4$, stained with FITC−cholera toxin B (CTxB), mounted and imaged with a Zeiss LSM 510 laser scanning confocal microscope for FITC (488_{exc}/BP 505-550_{em}) and rhodamine (568_{exc}/LP 585_{em}). Green channel, FITC-CTxb. Red channel, rhodamine. Scale bar represents 10 μm. Arbitrary units (a.u.).

Based upon the distribution of alk-16-labeled proteins to membrane compartments from Figure 5B, we evaluated the costaining of alk-16-labeled proteins with markers for the endoplasmic reticulum (ER), lysosomes and mitochondria using commercially available antibodies to calreticulin, lysosome-associated glycoprotein-1 (LAMP-1) and prohibitin, respectively. The comparative analysis with ER, lysosome and mitochondria markers demonstrates that alk-16-labeled proteins are not localized to one specific intracellular membrane compartment or dispersed throughout the cytoplasm but are distributed to several membrane-associated organelles, consistent with the notion that fatty-acylation targets proteins to membranes (Figure 6). The fluorescent imaging of fatty-acylated proteins by fluorescence microscopy and flow cytometry using chemical reporters therefore affords complementary means to in-gel fluorescence for analyzing protein fatty-acylation in cells.

Discussion

Installations of fatty acids onto proteins are fundamental posttranslational modifications that control a wide variety of biological pathways but has been challenging to study.[1] To improve the detection of protein fatty-acylation, we have synthesized fatty acid chemical reporters that allow rapid metabolic labeling of cells and robust fluorescence detection of fatty-acylated proteins using bioorthogonal labeling methods. While azido- and alkynyl-fatty acids both function as efficient chemical reporters, alkynyl-fatty acids in combination with azide-functionalized fluorophores afford the most sensitive mode for the detection of fatty-acylated proteins after click chemistry.

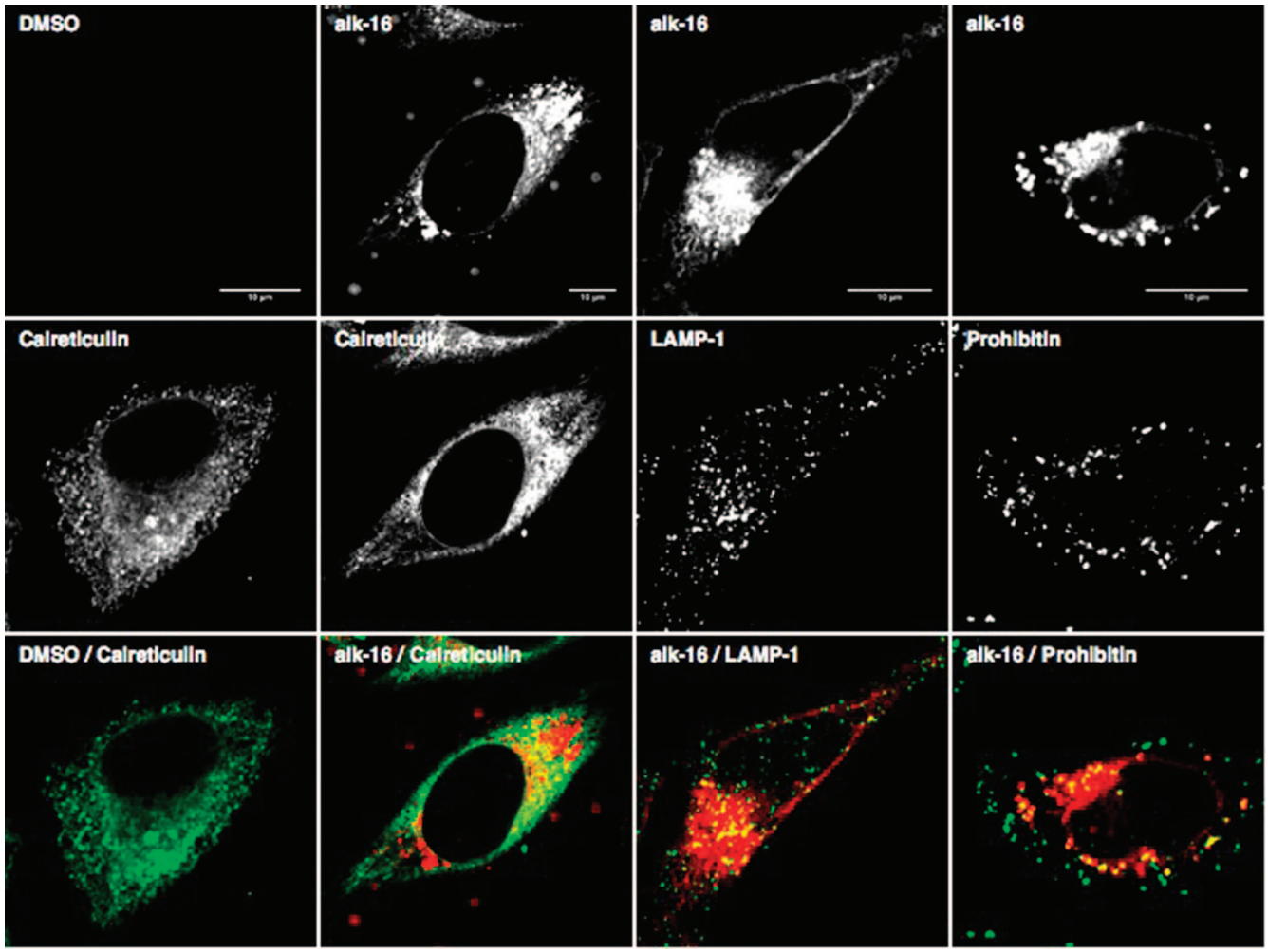

Figure 6. Analysis of protein fatty-acylation in cells by fluorescence microscopy. HeLa cells were metabolically labeled with DMSO or 20 μM alk-16 for 1 h, fixed with 3.7% PFA, permeabilized with 0.1% Triton X-100, reacted with 20 μM az-rho, 1 mM TCEP, 100 μM TBTA and 1 mM $CuSO_4$, stained with rabbit primary antibodies for cellular markers, followed by AlexaFluor647-conjugated goat anti-rabbit antibody, mounted and imaged with a Zeiss LSM 510 laser scanning confocal microscope for rhodamine (568_{exc}/BP 585-615_{em}) and AlexaFluor647 (633_{exc}/LP 650_{em}). Green channel, AlexaFluor647 anti-rabbit antibody. Red channel, rhodamine. Scale bar represents 10 μm.

The in-gel fluorescence detection of fatty-acylated proteins circumvents the need to transfer proteins onto membranes for immunoblotting, which can be problematic for hydrophobic polypeptides, and thus provides a more direct and quantitative means to analyze fatty-acylated proteins. The sensitivity of this chemical approach enables robust detection of fatty-acylated proteins expressed at endogenous levels within minutes after gel electrophoresis compared to days or weeks with radioactive analogues. In addition, fatty acid chemical reporters in conjunction with complementary fluorescent detection tags enable imaging and analysis of protein fatty-acylation in cells by fluorescence microscopy and flow cytometry. The robust fluorescence detection of fatty-acylated proteins with chemical reporters should therefore provide new opportunities to determine the dynamics of protein fatty-acylation by pulse-chase analysis of individual proteins, single cells as well as specific cell populations. In comparison to ABE, fatty acid chemical reporters afford a complementary approach for the analysis of *S*-acylated proteins that also enables the detection of non-thioester-linked fatty-acylated proteins such as *N*-myristoylated proteins as well as other potential sites of fatty-acylation on proteins. Moreover, bioorthogonal labeling methods also afford the opportunity to install affinity detection tags onto azide- or alkyne-modified substrates for enrichment and proteomic analysis of labeled proteins.[26,27] Indeed, while this manuscript was under review Martin and Cravatt described the proteomic analysis of fatty-acylated proteins using alk-16 or 17-ODYA.[39] We have also performed proteomic analyses of azido- and alkynyl-fatty acid-labeled proteins that will be described elsewhere. In summary, the advances described here present significant improvements in the detection of protein fatty-acylation with chemical reporters compared to previously reported methods[16−21] and present new opportunities to dissect the functions and regulatory mechanisms of protein fatty-acylation in physiology and disease. Finally, the alkynyl-fatty acids reported here contribute to the growing list of chemical tools for studying nucleic acid[40,41] and protein synthesis[42,43] as well as other posttranslational modifications[44] in cells.

Experimental Methods

Metabolic Labeling. Jurkat cells (human T lymphoma) were cultured in RPMI medium 1640 supplemented with 10% fetal

(39) Martin, B. R.; Cravatt, B. F. *Nat. Methods* **2009**, *6*, 135–8.
(40) Salic, A.; Mitchison, T. J. *Proc. Natl. Acad. Sci. U.S.A.* **2008**, *105*, 2415–2420.

bovine serum (FBS), 100 U/mL penicillin and 100 μg/mL streptomycin. HeLa, 3T3 and DC2.4 cells were cultured in DMEM, supplemented with 10% fetal bovine serum (FBS), 100 U/mL penicillin and 100 μg/mL streptomycin. Cells were maintained in a humidified 37 °C incubator with 5% CO_2. Trypan blue exclusion was used to determine cell viability. Cells were treated with either az-12, az-15, alk-12, alk-14 or alk-16 at concentrations described from 50 mM DMSO stock solutions using the corresponding media for the respective cell types. The same volume of DMSO was used in the negative control. For coincubation with inhibitors, Jurkat cells were pretreated with cycloheximide (CHX) (10 μM, 100 mM stock solution in DMSO), 2-hydroxymyristic acid (HMA) (1 mM, 100 mM stock solution in DMSO) or 2-bromopalmitate (2-BP) (50 μM, 30 mM stock solution in DMSO) prior to metabolic labeling. Fatty acid-free 1% BSA (Sigma) was added to the medium in the case of HMA treatment. After 30 min of preincubation at 37 °C, alk-12, alk-14 or alk-16 (20 μM, 50 mM stock solution in DMSO) was added to the medium. Following metabolic labeling, cells were harvested, washed once with ice-cold PBS and pelleted at 1000*g* for 5 min. Cells were directly lysed or flash frozen in liquid nitrogen and stored at −80 °C prior to lysis. No significant loss of signal was observed for frozen cell pellets.

Preparation of Cell Lysates. Cell pellets obtained from 10 × 10^6 Jurkat cells or 1 confluent well of a 6-well plate of HeLa, 3T3 or DC2.4 cells were lysed with 100 μL of ice-cold modified RIPA lysis buffer (1% Nonidet P 40, 1% sodium deoxycholate, 0.1% SDS, 50 mM triethanolamine pH 7.4, 150 mM NaCl, 5× EDTA-free Roche protease inhibitor cocktail, 10 mM phenylmethylsulfonyl fluoride (PMSF)). Cell lysates were collected after centrifuging at 1000*g* for 5 min at 4 °C to remove cell debris. Protein concentration was determined by the BCA assay (Pierce). Typical lysate protein concentrations obtained: Jurkat 2−3 mg/mL, HeLa 1−2 mg/mL, 3T3 0.5−1 mg/mL and DC2.4 1−2 mg/mL. Cell lysates were diluted with modified RIPA lysis buffer to achieve final protein concentration of ∼1 mg/mL for labeling reactions.

Staudinger Ligation. Cell lysates (50 μg) in 46.5 μL modified RIPA lysis buffer were reacted with 1 μL phosphine-biotin[45] (200 μM, 10 mM stock solution in DMSO) and 2.5 μL DTT (5 mM, 100 mM stock solution in deionized water) for a total reaction volume of 50 μL for 1 h at room temperature. DTT prevents nonspecific oxidation of phosphine-biotin, which can increase levels of background labeling. The reactions were terminated by the addition of −20 °C methanol (1 mL), placed at −80 °C overnight and centrifuged at 18000*g* for 10 min at 0 °C to precipitate proteins. The supernatant from the samples was discarded. The protein pellets were allowed to air-dry for 10 min, resuspended in 35 μL of resuspension buffer (4% SDS, 50 mM triethanolamine pH 7.4, 150 mM NaCl), diluted with 12.5 μL 4× reducing SDS-loading buffer (40% glycerol, 200 mM Tris-HCl pH 6.8, 8% SDS, 0.4% bromophenol blue) and 2.5 μL 2-mercaptoethanol, heated for 5 min at 95 °C and ∼20 μg of protein was loaded per gel lane for separation by SDS-PAGE (10% or 4−20% Bio-Rad Criterion Tris-HCl gel).

Cu^I-Catalyzed Huisgen [3 + 2] Cycloaddition/Click Chemistry. Cell lysates (50 μg) in 47 μL modified RIPA lysis buffer were reacted with 3 μL freshly premixed click chemistry reaction cocktail [azido- or alkynyl-detection tag (100 μM, 10 mM stock solution in DMSO), tris(2-carboxyethyl)phosphine hydrochloride (TCEP) (1 mM, 50 mM freshly prepared stock solution in deionized water), tris[(1-benzyl-1*H*-1,2,3-triazol-4-yl)methyl]amine (TBTA) (100 μM, 10 mM stock solution in DMSO) and $CuSO_4 \cdot 5H_2O$ (1 mM, 50 mM freshly prepared stock solution in deionized water)] for a total reaction volume of 50 μL for 1 h at room temperature. The reactions were terminated by the addition of ice-cold methanol (1 mL), placed at −80 °C overnight and centrifuged at 18000*g* for 10 min at 4 °C to precipitate proteins. The supernatant from the samples was discarded. The protein pellets were allowed to air-dry for 10 min, resuspended in 35 μL of resuspension buffer (4% SDS, 50 mM triethanolamine pH 7.4, 150 mM NaCl), diluted with 12.5 μL 4× reducing SDS-loading buffer (40% glycerol, 200 mM Tris-HCl pH 6.8, 8% SDS, 0.4% bromophenol blue) and 2.5 μL 2-mercaptoethanol and heated for 5 min at 95 °C; ∼20 μg of protein was loaded per gel lane for separation by SDS-PAGE (10% or 4−20% Bio-Rad Criterion Tris-HCl gel).

Immunoprecipitation. Cell pellets obtained from 15 × 10^6 Jurkat cells or transfected HeLa cells were lysed with 50 mL of ice-cold Brij lysis buffer (1% Brij 97, 50 mM triethanolamine pH 7.4, 150 mM NaCl, 5× EDTA-free Roche protease inhibitor cocktail, 10 mM PMSF). Cell lysates were collected after centrifuging at 1000*g* for 5 min at 4 °C to remove cell debris. Protein concentration was determined by the BCA assay (Pierce). Typical lysate protein concentration obtained: 6−8 mg/mL. LAT, Lck and Ras proteins were immunoprecipitated from 200 μg Jurkat cell lysate using the following antibodies at recommended concentrations: mouse anti-Lck ($p56^{lck}$) monoclonal (Clone 3A5, Thermo Scientific), rat anti-v-H-ras (Ab-1) monoclonal (Y13-259 agarose conjugate, Calbiochem), and rabbit anti-LAT polyclonal (Upstate). For Fyn analysis, HeLa cells were grown in 10 cm dishes to approximately 90% confluence in DMEM, supplemented with 10% FBS, and transfected with wild type, G2A or C3,6S Fyn constructs using Lipofectamine 2000 (Invitrogen). The human Fyn constructs, wild-type and mutant Fyn cDNAs cloned into eukaryotic expression vector pCMV5, were gifts from Dr. Marilyn Resh, Memorial Sloan-Kettering Cancer Center. The following day, cells were metabolically labeled with alkynyl-fatty acid analogues as described above. A rabbit anti-Fyn polyclonal (Upstate) was used to immunoprecipitate wild-type and mutant Fyn proteins from transfected and metabolically labeled HeLa cells. Twenty-five microliters of packed protein A-agarose beads (Roche) was used per sample. Upon incubation at 4 °C for an hour with an end-over-end rotator (Barnstead/Thermolyne), the beads were washed thrice with ice-cold modified RIPA lysis buffer (1% Triton X-100, 1% sodium deoxycholate, 0.1% SDS, 10 mM Tris pH 7.4, 150 mM NaCl). The beads were resuspended in 20 μL of resuspension buffer (4% SDS, 50 mM triethanolamine pH 7.4, 150 mM NaCl) and freshly premixed click chemistry reagents (same as above) were added. After 1 h at room temperature, the reaction mixture was diluted with 6.7 μL 4× reducing SDS-loading buffer (40% glycerol, 200 mM Tris-HCl pH 6.8, 8% SDS, 0.4% bromophenol blue) and 1.3 μL 2-mercaptoethanol, heated for 5 min at 95 °C, and 20 μL of the supernatant was loaded per gel lane for separation by SDS-PAGE (4−20% Bio-Rad Criterion Tris-HCl gel).

Hydroxylamine Treatment of Gels. After the proteins were separated by SDS-PAGE, the gel was soaked in 40% MeOH, 10% acetic acid, shaking overnight at room temperature, washed with deionized water (2 × 5 min) and scanned for the prehydroxylamine treatment fluorescence. The gel was then soaked in PBS, shaking 1 h at room temperature, followed by soaking in 1 M NH_2OH (pH 7.4), shaking 8 h at room temperature, washing with deionized water (2 × 5 min), and soaking in 40% MeOH, 10% acetic acid, shaking overnight at room temperature. The gel was washed with deionized water (2 × 5 min) and scanned for the post-hydroxylamine treatment fluorescence.

In-gel Fluorescence Scanning. Proteins separated by SDS-PAGE were visualized by first soaking the gel in 40% MeOH, 10% acetic acid with shaking for 5 min, followed by soaking in deionized water with shaking for 5 min and directly scanning the gel on an

(41) Jao, C. Y.; Salic, A. *Proc. Natl. Acad. Sci. U.S.A.* **2008**, *105*, 15779–15784.
(42) Link, A. J.; Mock, M. L.; Tirrell, D. A. *Curr. Opin. Biotechnol.* **2003**, *14*, 603–609.
(43) Wang, L.; Xie, J.; Schultz, P. G. *Annu. Rev. Biophys. Biomol. Struct.* **2006**, *35*, 225–249.
(44) Prescher, J. A.; Bertozzi, C. R. *Nat. Chem. Biol.* **2005**, *1*, 13–21.
(45) Vocadlo, D. J.; Hang, H. C.; Kim, E. J.; Hanover, J. A.; Bertozzi, C. R. *Proc. Natl. Acad. Sci. U.S.A.* **2003**, *100*, 9116–9121.

Amersham Biosciences Typhoon 9400 variable mode imager (excitation 532 nm, 580 nm filter, 30 nm band-pass).

Immunoblotting. Proteins separated by SDS-PAGE were transferred (50 mM Tris, 40 mM glycine, 0.0375% SDS, 20% MeOH in deionized water, Bio-Rad Trans-Blot Semi-Dry Cell, 20 V, 1 h) onto a PVDF membrane which was blocked (5% nonfat dried milk, 1% BSA and 0.1% Tween-20 in PBS) for 1 h at 25 °C or overnight at 4 °C. The membrane was washed thrice with PBST (0.1% Tween-20 in PBS), incubated with streptavidin−horseradish peroxidase (1 mg/mL diluted 1:25,000 in PBST, Pierce), and subsequently developed with ECL Western blotting detection reagents (Amersham). Alternatively, Lck, LAT, Ras and Fyn protein levels were visualized by incubating the blots at recommended concentrations in 5% casein, 1% BSA in PBST with mouse anti-Lck ($p56^{lck}$) monoclonal (Clone 3A5, Thermo Scientific), mouse anti-LAT monoclonal (2E9, Upstate), mouse anti-Ras monoclonal (RAS10, Upstate) or mouse anti-Fyn monoclonal (S1, Chemicon), respectively, followed by a goat anti-mouse-HRP conjugated secondary antibody (Upstate) in the blocking buffer mentioned above.

Fluorescence Imaging. HeLa cells were cultured on sterile coverslips in DMEM, supplemented with 10% fetal bovine serum (FBS), 100 U/mL penicillin, and 100 μg/mL streptomycin and maintained in a humidified 37 °C incubator with 5% CO_2. Cells were treated with either az-12, az-15, alk-12, or alk-16 (20 μM, 50 mM stock solution in DMSO) in DMEM supplemented with 2% FBS, 100 U/mL penicillin, and 100 μg/mL streptomycin. The same volume of DMSO was used as a negative control. After 1 h of labeling at 37 °C, the cells were washed once with warm PBS, fixed (3.7% PFA in PBS for 10 min at room temperature), and washed twice with ice-cold PBS. The cells were permeabilized (1% Tween-20 or 0.1% Triton X-100 in PBS for 10 min at room temperature or −20 °C MeOH for 10 min) or not permeabilized and washed with PBS (3 × 5 min with gentle agitation). Cells were blocked (10% FBS, 50 mg/mL sucrose, 20 mg/mL BSA) for 30 min at room temperature and washed with PBS (3 × 5 min with gentle agitation). The cells were then treated with a freshly premixed click chemistry reaction solution [alk-rho or az-rho (20 μM, 10 mM stock solution in DMSO), TCEP (1 mM, 50 mM freshly prepared stock solution in deionized water), TBTA (100 μM, 10 mM stock solution in DMSO), and $CuSO_4 \cdot 5H_2O$ (1 mM, 50 mM freshly prepared stock solution in deionized water)] in PBST (0.1% Tween-20) for 1 h at room temperature. The cells were washed (3 × 5 min with gentle agitation in 1% Tween-20 and 0.5 mM EDTA in PBS, followed by 2 × 5 min with gentle agitation in PBS), and the samples were ready for secondary labeling. Throughout the experiment, detergents were omitted for samples not permeabilized. The cells were then incubated for 30 min in PBS with 5 μg/mL FITC-conjugated cholera toxin B (FITC-CTxB, Sigma) or 1 h in 1% BSA in PBST with rabbit anti-calreticulin polyclonal (ab2907, Abcam), rabbit anti-LAMP1 polyclonal (ab24170, Abcam) or rabbit anti-prohibitin polyclonal (ab28172, Abcam), and washed with PBS (3 × 5 min with gentle agitation). Samples labeled with rabbit antibodies were then labeled with AlexaFluor647-conjugated goat anti-rabbit IgG (H+L) (2 mg/mL diluted 1:1000 in 1% BSA in PBST, Invitrogen), and a final wash with PBS (3 × 5 min with gentle agitation) before mounting (ProLong Gold, Invitrogen). Wide-field images were taken on a Zeiss Axioplan2 wide-field microscope equipped with a Fluar 10×/0.50 air objective and a LP 585 nm filter. Confocal images were collected using a Zeiss LSM 510 laser scanning confocal microscope equipped with a Plan-Apochromat 100×/1.40 oil objective. FITC and rhodamine were excited with a krypton/argon laser at 488 nm and 568 nm, respectively, and the emission was collected through a BP 505-550 and 585-615 nm filters, respectively. AlexaFluor647 was excited with a HeNe laser at 633 nm, and the emission was collected through a LP 650 nm filter.

Flow Cytometry. HeLa cells were labeled with DMSO or alk-16 for 1 h at 20 and 100 μM. Cells were harvested and washed once with cold PBS and fixed with 3.7% PFA in PBS for 10 min. Cells were washed once with 2% FBS in PBS followed by permeabilization (1% Tween-20 or 0.1% Triton X-100 in PBS for 10 min at room temperature or −20 °C MeOH for 10 min) or no permeabilization. Cells were washed with PBS and blocked for 10 min (2% FBS in PBS). Click chemistry was performed in 100 μL PBS containing 20 μM az-rho, 1 mM TCEP, 100 μM TBTA, and 1 mM $CuSO_4 \cdot 5H_2O$. Cells were washed five times with 1% Tween-20 and 0.5 mM EDTA in PBS and once with 2% FBS in PBS. Flow cytometry analysis were performed on Beckton Dickinson LSRII machine equipped with a 488 nm excitation laser and a filter set consisting of a 550 nm long pass filter and a 575/26 nm detection filter. Cellular debris was eliminated from analysis based on forward and side-scatter measurements. Singlets were gated, based on side-scatter area versus width. Histograms were generated using FloJo analysis software.

Acknowledgment. We thank Prof. Marilyn Resh (Memorial Sloan-Kettering Cancer Center) for generously providing Fyn constructs and helpful advice. H.C.H. acknowledges support from The Rockefeller University, Irma T. Hirschl/Monique Weill-Caulier Trust, and Ellison Medical Foundation. G.C. thanks the Rockefeller/Sloan-Kettering/Cornell Tri-Institutional Program in Chemical Biology. M.M.Z. is supported by A*STAR, Singapore. J.S.Y. is supported by the Irving Institute Fellowship Program of the Cancer Research Institute. A.S.R. thanks the New York Community Trust-Heiser Grant for a postdoctoral fellowship. E.S. thanks The Rockefeller University SURF program for an undergraduate fellowship.

Supporting Information Available: Synthetic methods and supplementary figures. This material is available free of charge via the Internet at http://pubs.acs.org.

JA810122F